5. Compact Binaries

https://doi.org/10.1017/S0252921100012318 Published online by Cambridge University Press

AN EXOSAT OBSERVATION OF SPECTRAL VARIABILITY FROM THE RS CVn BINARY AR LAC

N.E. White[1], R.A. Shafer[1,2], A.N. Parmar[1], K. Horne[3], and J.L. Culhane[4]

[1] EXOSAT Observatory, ESTEC, Noordwijk, The Netherlands

[2] present address: GSFC, Greenbelt, Maryland, USA

[3] Space Telescope Science Institute, Baltimore, Maryland, USA.

[4] Mullard Space Science Laboratory, Holmbury St Mary, Surrey, UK.

ABSTRACT. The eclipsing RS CVn system AR Lac (G2IV+K0IV) has been observed continuously for one 2 day binary cycle with the EXOSAT observatory. Below 1 keV a factor of two intensity modulation is seen with a flat bottomed minimum around the time of primary eclipse and a shallow dip preceeding primary eclipse. Above 1 keV, where only emission with temperatures $> 10^7$ K would be detected, no orbital modulation or eclipse is seen. This suggests that the > 20 million degree emission comes from a large region, comparable in size to the binary seperation. The modulation in the < 1 keV lightcurve has been modelled by χ^2 fitting to X-ray bright spots and by using maximum entropy deconvolution. The lower temperature emission is found to orginate in compact regions with a pressure and temperature similar to that of the flaring sun.

1. INTRODUCTION

The close proximity of the sun allows the luxury of imaging individual magnetic loop structures. For other stars the three dimensional spatial distribution of the X-ray emitting corona must be mapped indirectly by observing through an eclipse of the corona by a binary companion, or by searching for a rotational modulation caused by the self-eclipse of active regions by the underlying star. The RS CVn binaries show extreme coronal activity and are ideal for eclipse and rotational modulation investigations. They typically have orbital periods in the range 1 to 14 day with the hotter component of spectral type F-G and luminosity class IV-V. The cooler, usually more evolved component is typically K0IV. A characteristic feature of these systems is a low-amplitude optical modulation at the orbital period caused by giant star spots on the stellar surface, analogous to sun spots (e.g. Eaton and Hall 1979). Orbital phase dependent features found in rotationally broadened absorption and emission line profiles can be used to locate, respectively, dark starspots and regions of enhanced chromospheric emission (Vogt and Penrod 1983, Walter et al 1987).

A spectral survey of the quiescent spectral properties of seven RS CVn's by Swank et al (1981) using the *Einstein* SSS showed at least two distinct temperatures distributions to be present of $4 - 8 \times 10^6$ K and $\geq 2 \times 10^7$ K. The emission measures of both components are similar and within the range $10^{53} - 10^{54}$ cm^{-3}. Swank et al (1981) suggest that the bimodal temperature distribution indicates two isothermal families of magnetic loops, with possibly, different dimensions and pressures. The spectra of luminous late type stars in the Hyades taken by the *Einstein* imaging proportional counter (IPC) are well fit by a single family of loops, with a continuous temperature

https://doi.org/10.1017/S0252921100012318 Published online by Cambridge University Press

distribution and a maximum temperature at the loop apex of $\sim 10^7$ K (Stern, Antiochos, and Harnden 1986). A two temperature model also provides an acceptable fit. This suggested that detectors with strong structure in their energy efficiency (e.g. the carbon absorption edge in the IPC response) and poor energy resolution may artificially create a two temperature distribution (Majer et al 1986). However, EXOSAT transmission grating spectra of two RS CVn systems are only well fit by a two temperature model. The Stern et al (1986) single loop model was excluded. If a solar loop model is relevant then Mewe et al (1986) require at least two families of loops with apex temperatures of $\sim 5\times10^6$ K and $>10^7$ K. The EXOSAT grating spectra do not show any evidence for emission with a temperature of 1-2 million degrees expected from close to the base of the loops. This requires that the cross section of the loops expand rapidly above the stellar surface. The EXOSAT grating spectra clearly demonstrate that the ability to make unambiguous comparisons between loop models requires observations taken with sufficient spectral resolution to resolve temperature sensitive line complexes.

AR Lac is a 1.98 day period eclipsing RS CVn system containing a G2IV primary and a K0IV secondary with radii of 1.54 $R_\odot$ and 2.81 $R_\odot$ respectively, and a seperation of 9.22 $R_\odot$ (Chambliss 1976). The combination of a close to 90° inclination, relatively short orbital period, nearby distance of 50 pc and high X-ray luminosity of 10^{31} erg s^{-1} make AR Lac a prime candidate for an eclipse/rotational modulation study. Walter, Gibson and Basri (1983) observed over one orbital cycle using the *Einstein* observatory but only with an orbital phase coverage of $\sim$ 17 %. Minima seen around the time of primary and secondary eclipse could be modelled as due to the eclipse of compact regions on each star and one extended region on the K subgiant.

The highly elliptical 90hr earth orbit of the European Space Agency's X-ray astronomy observatory EXOSAT gave for the first time the possibility to obtain uniterrupted X-ray light curves for up to ~76hr (White and Peacock 1988 and refs therein). This paper presents an uninterupted EXOSAT observation over one complete orbital cycle of AR Lac with an orbital phase coverage of close to 100%. We consider in detail the location, height and temperature of the corona in AR Lac.

2. OBSERVATION AND RESULTS

The EXOSAT observation of AR Lac began at UT 1300 on 1984 July 3 and ended at the same time two days later. These times correspond to orbital phases, ϕ, from 310° to 685°, where $\phi = 360°$ is the center of primary eclipse. This assumes an ephemeris for the interval 1983–1985 of JD Hel. 2,445,611.6290 + 1.98316E provided by M. Rodono (1988, Priv. communication). Two instruments were used. The low energy imaging telescope (LEIT) with a channel multiplier array and a 4000Å filter (0.05 – 2keV) and the medium energy (ME) proportional counter array (1 – 30keV). The response of these two instruments are nicely matched to the spectra of the two temperature components found by Swank et al (1981). The ME is sensitive only to the higher temperature component, the LEIT is sensitive to both.

The background subtracted lightcurves from the ME and LEIT are shown in Figure 1. The duration of the two eclipses, from 1^{st} to 4^{th} contact, are indicated by horizontal lines. The most striking feature of the LEIT light curve is a minimum lasting ~12hrs centered on the time of primary eclipse, where a factor of two reduction in count rate occurs. There is also a shallow minimum preceeding the time of secondary eclipse. In the ME the most prominent feature is a flare at the beginning of the observation that lasted for ~2hr. The ME lightcurve shows no evidence for features that might be identified with the eclipses and, in particular, no minimum is seen at the time of primary eclipse corresponding to that seen in the LEIT. There is some low level variability in the ME, with a second smaller flare following secondary eclipse. Both flares are also seen in the LEIT.

Background subtracted spectra from the ME have been accumulated for five different intervals during the observation. The first interval, lasting 2hr, only includes the large flare that occured

at the beginning of the observation. The other four spectra have accumulation times of between 8 and 13 hr and cover the remainder of the observation. A significant signal is detected only between 1.5 and 6.0 keV. The flare spectrum has been obtained by subtracting the following source plus background data. This spectrum represents the average over the whole flare which had a very similar rise and decay time of $\sim$ 30 min. The decay overlaps the time of primary eclipse and it is possible that part of the decay was caused by the flaring region being eclipsed by the companion star.

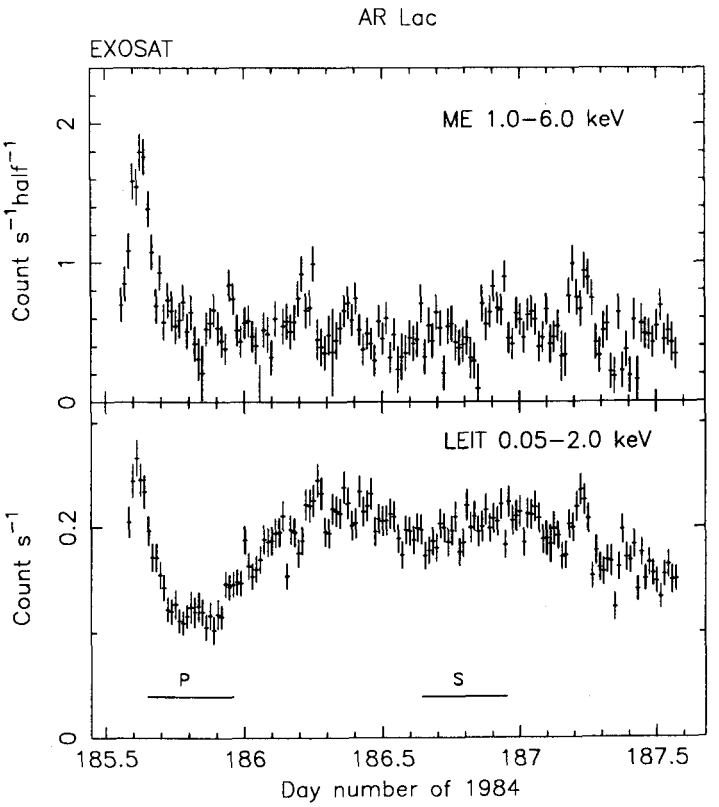

Figure 1. The light curve of AR Lac. The accumulation time is 1200s. The two horizontal lines indicate the time from 1^{st} to 4^{th} contact for primary (P) and secondary (S) eclipses.

The results for the quiescent cases are all similar with a temperature of 1.4×10^7 K and an emission measure of 5×10^{53} cm^{-3}. This is respectively a factor of $\sim$ 3 and $\sim$ 6 lower than the two values reported in Swank et al (1981). The ME flare spectrum has a temperature of 4.5×10^7 K and an emission measure of 4×10^{53} cm^{-3}. The emission measure of the low temperature component and the line of sight interstellar absorption to AR Lac can be constrained by including the LEIT lexan 4000Å filter count rate in the spectral fitting. The temperature of the low temperature component could not be usefully constrained. If it is fixed at $5.0 - 7.0 \times 10^6$ K (Swank et al 1981) then $N_H < 1.3 \times 10^{20}$ H cm^{-2}. The emission measure depends on orbital phase and is $< 5.0 \times 10^{53}$ cm^{-3} and $< 2.5 \times 10^{53}$ cm^{-3} for the maximum and minimum of the modulation. A lower limit to the emission measure comes from the LEIT modulation which requires that the diference between the peak and minimum counting rate comes from a component with a temperature $< 10^7$ K. This corresponds

https://doi.org/10.1017/S0252921100012318 Published online by Cambridge University Press

to a minimum emission measure of 2×10^{53} cm^{-3}, which in turn requires N_H to be $> 1 \times 10^{19}$ H cm^{-2}.

3. ECLIPSE MODELLING

The primary objectives are to 1) determine the maximum fraction of the stellar surface covered by an X-ray emitting corona, 2) set limits on the vertical extension above the stellar surface of the X-ray emitting structures, and 3) to locate where the X-ray structures are on the surface of the two stars. We have modelled the LEIT lightcurve both by χ^2 fitting to uniformly emitting structures on one or both of the stars and using a maximum entropy technique. All the non-flaring features in the LEIT lightcurve are be assumed to be the result of either an eclipse by the companion star or a rotational modulation. The X-ray lightcurve recorded by the ME shows two flares and also many small fluctuations, but no overall orbital modulation or eclipses. This precludes any useful eclipse modelling of the ME lightcurve.

The total count rate in the LEIT will be a combination of the 15×10^6 K component seen in ME, plus that from the 7×10^6 K component. The contribution of the hotter component to the LEIT can be estimated from the spectrum measured by the ME, but depends on the interstellar absorption. The range of N_H found in the previous sub-section predicts that the hot component will contribute between 30 and 100% of the LEIT counting rate during primary eclipse. A d.c. component was included as a free parameter to account for the unmodulated contribution to the LEIT counting from the hot component.

Acceptable fits to the LEIT lightcurve are obtained for only two structures, but with multiple solutions caused by ambiguity as to which star they are on. Three different permutations are possible: *Case 1*, the G star is X-ray bright and the K star is dark; *Case 2*, the G star is dark and the K star is bright; *Case 3*, both the G and the K stars are bright. The best fits with two structures require the height of one to be an order of magnitude larger than the other. The significance of this was tested by repeating the fit, but with the height of all the structures the same. In some models a third structure was then required to obtain an acceptable fit. A total of eight different models were tried. The height and the covering fraction are very similar for all eight models, only the locations change. We illustrate two representative fits for case 3 in Figures 2 and 3. Each structure is labeled by the spectral type of the underlying star and its longitude, e.g. G180. Zero longitude corresponds to the central meridians on the G and K stars at primary eclipse and increases in the same sense as increasing orbital phase.

The Maximum Entropy Method (MEM) models the X-ray light curve by distributing the coronal X-ray emission as uniformly as possible over the stellar surfaces. This approach complements the χ^2 fitting because the broad class of all possible positive X-ray maps fall within the scope of MEM and it can be used to investigate if it is possible to fit the data with a larger covering fraction. MEM maps were fitted to the observed X-ray light curve with the aid of the iterative fitting program MEMSYS, which uses an algorithm similar to that described by Skilling and Bryan (1984). MEM maps were generated for each of the models found from the χ^2 fitting. The coronal height and the d.c. background intensity levels were set at their best-fit values. The covering fraction $f(p)$ is defined as the fraction of the stellar surface enclosed by the surface brightness contour that encloses a fraction p of the total X-ray flux. The contour levels used in the Figures are not equally spaced in surface brightness, but instead they enclose the fractions $p =$ 0.1, 0.3, 0.5, 0.7 and 0.9 of the total flux. The latter two contour levels are given as dashed lines. Above each map the surface area of each star responsible for 50% and 90% of the total emission are given. We concentrate on the maps made assuming both stars are bright and these are shown in Figures 4 and 5.

The map shown in Figure 4 assumes the coronal height on the K star is small (0.04 $R_\odot$), but that on the G star it is 1.5 $R_\odot$, as given by the χ^2 fitting. The cluster of three bright regions at high

https://doi.org/10.1017/S0252921100012318 Published online by Cambridge University Press

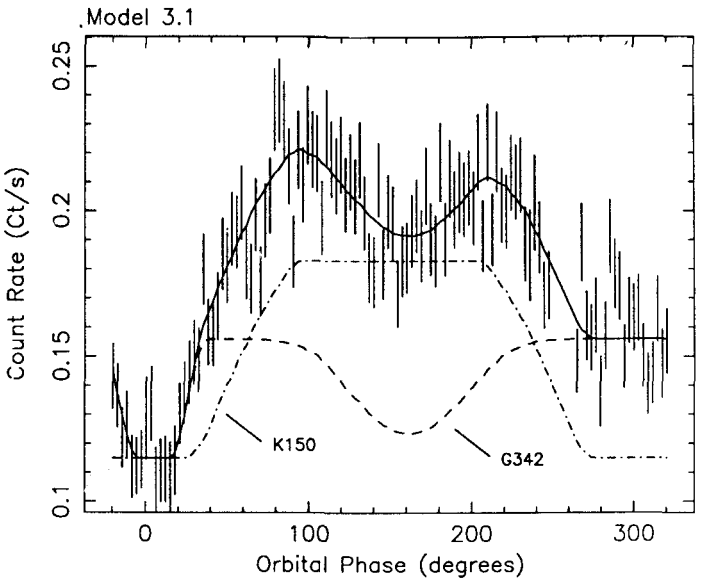

Figure 2. The best fit to the LEIT light curve for two uniformly emitting spots, with one on each star. The G star structure is extended with a height, H, of $1.5R_\odot$ and the K star structure compact with H< 0.05 $R_\odot$. The dashed lines show the contributions of the individual lightcurves to the total. Two flares have been excluded.

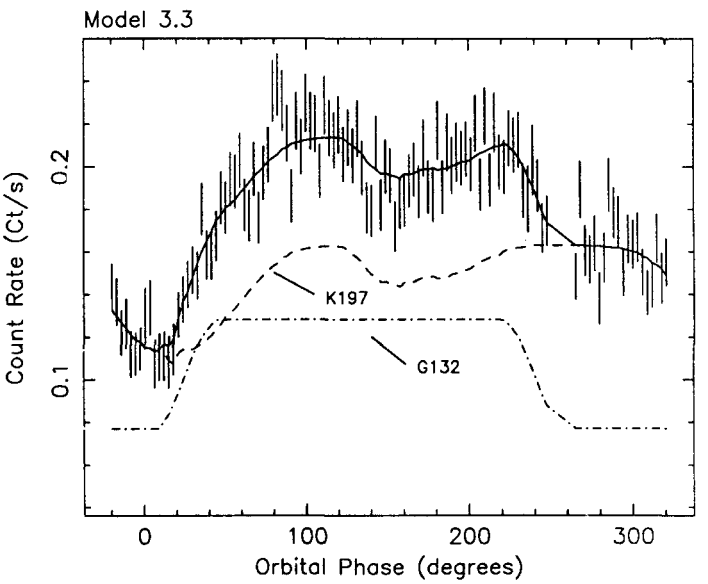

Figure 3. The same as Figure 2, but with the extended structure on the K star with H=4.0 $R_\odot$ and the compact structure on the G star with H< 0.09 $R_\odot$.

https://doi.org/10.1017/S0252921100012318 Published online by Cambridge University Press

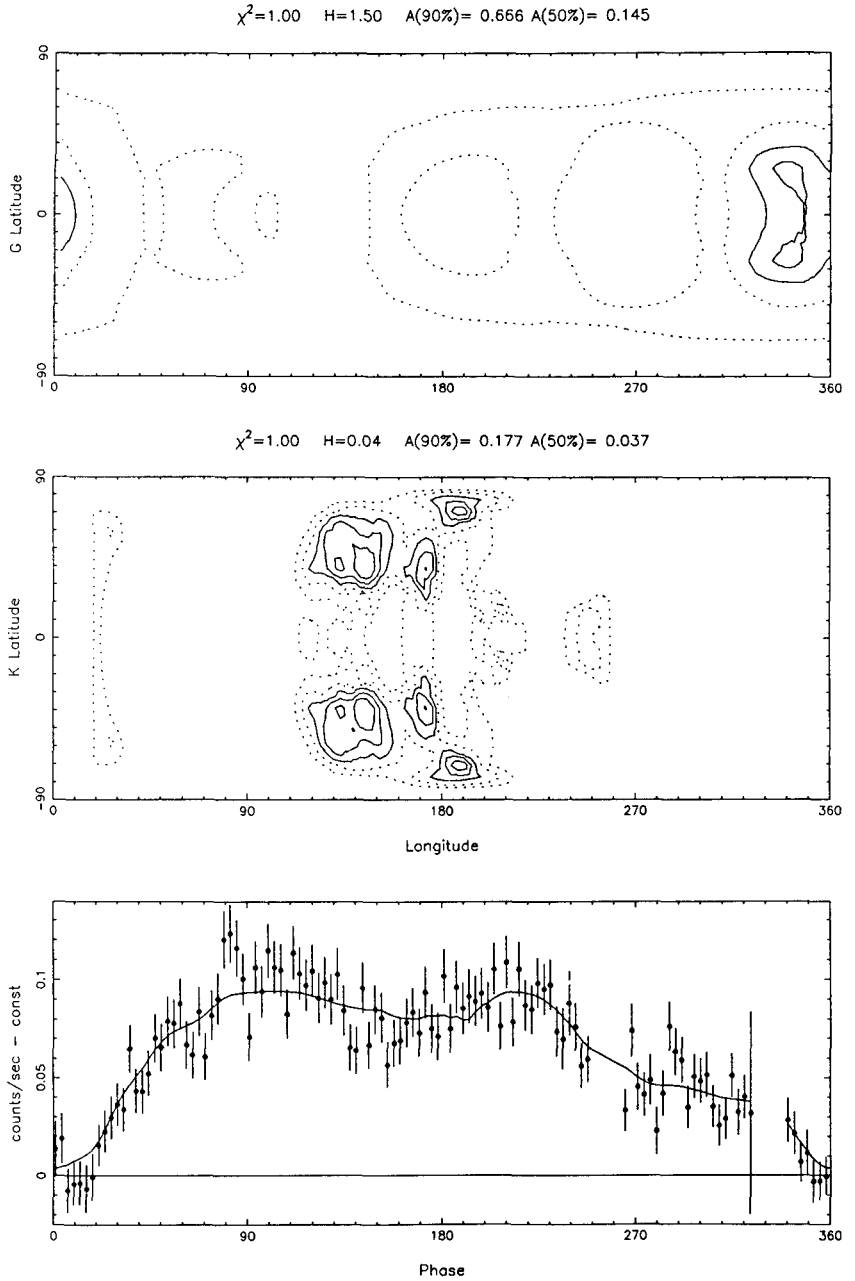

Figure 4. The MEM map generated under the assumption that both stars are X-ray bright. The top panel shows the G star map and the lower panel the K star map. The coronal height on the G star was assumed to be 1.5 $R_\odot$ and on the K star 0.04 $R_\odot$. The contours give pressure isobars of 1.9, 3.4, 5.1, 6.7 and 8.6 dyne cm^{-2} on the K star and 17, 31, 47, 61 and 79 dyne cm^{-2} on the G star. The dashed contours distinguish the two lowest pressures.

https://doi.org/10.1017/S0252921100012318 Published online by Cambridge University Press

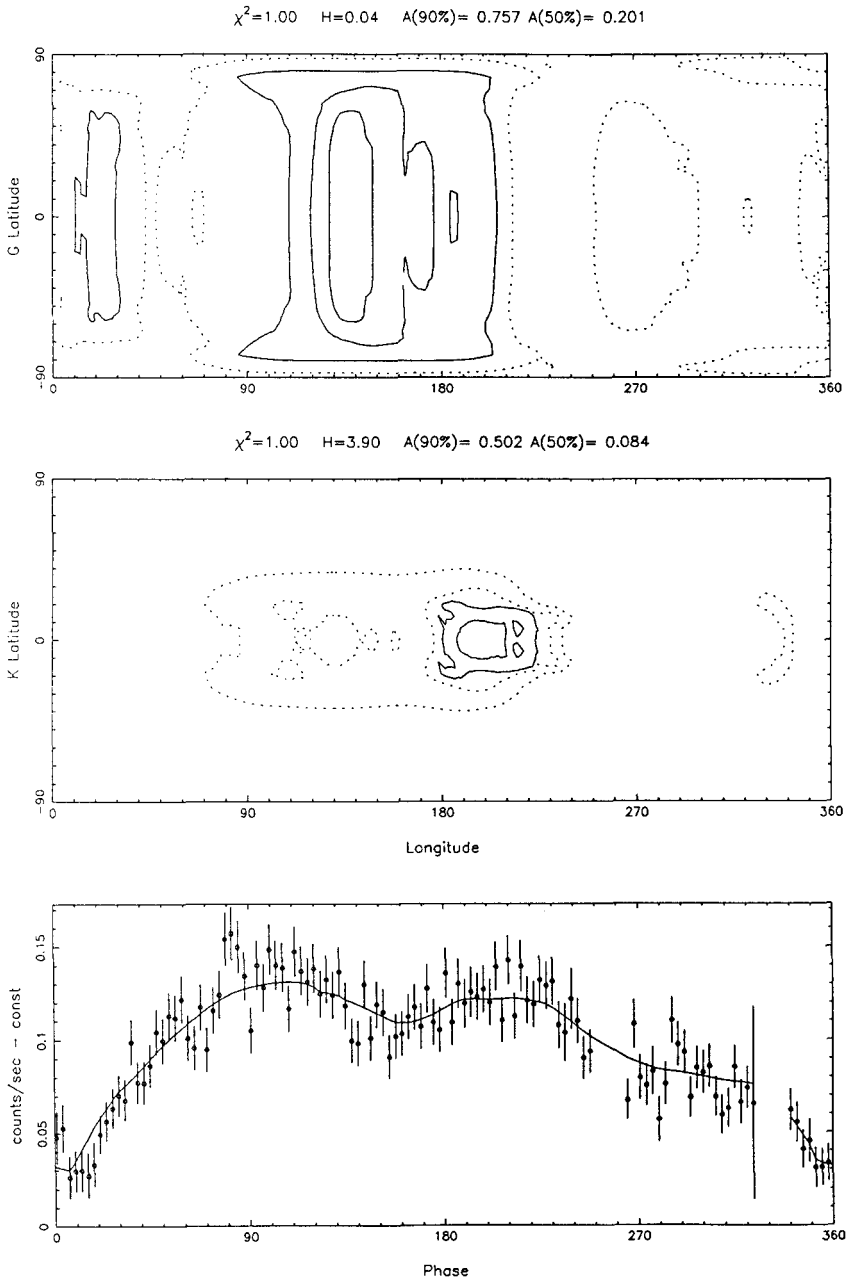

Figure 5. The MEM map generated under the assumption that both stars are X-ray bright and that the coronal height on the K star is 3.9 $R_\odot$ and on the G star 0.04 $R_\odot$. The contours give pressure isobars of 18, 31, 39, 59 and 77 dyne cm^{-2} on the G star and 1.0, 1.8, 2.3, 3.5 and 4.5 dyne cm^{-2} on the K star.

https://doi.org/10.1017/S0252921100012318 Published online by Cambridge University Press

latitudes on the K star between longitudes of 120-200° matches up with K150 in χ^2 modelling. Similarly on the G star the structure near the equator at $\sim$ 340° corresponds nicely with G340. In Figure 5 the K star corona is extended with $H_2 = 3.9$, and the G star corona is compact with $H_1 = 0.04$, the values given by the χ^2 fitting. There is a prominent structure on the equator of the K star at a longitude of 200°. This corresponds to region K215 in Figure 3. This tall spot protrudes so far above the stellar surface that its eclipse by the G star is displaced in phase and so gives the broad minimum centered on phase 160°. The G star flux remains high with the primary eclipse caused by a region at a longitude of 25°. There is also a structure on the G star at a longitude of 140°, which matches well with the region G138.

Because the inclination of AR Lac is 90°, we cannot distinguish between north or south latitudes. In addition, the latitude is usually only constrained to be either high or low. If the structures are on the G star then their latitude is < 50°. If the structures are on the K star then they are, with one exception, always between 40° and 80°. The exception is an extended structure at a longitude of $\sim$ 210°. This must be at a low latitudes on the K star, otherwise the flux in the d.c. component is less than expected from the extrapolation of the hot component.

All the models require at least one compact X-ray emitting structure on one of the stars. The height of this compact structure is only marginally resolved and because of this we will treat all of the measurements as upper limits. If the structures are all on the G star, or on both the G and the K star, then H < 0.04 $R_\odot$ (< 7×10^9 cm). This increases to < 0.17 $R_\odot$ (< 1×10^{10} cm) if they are only on the K star. If the height of individual structures are allowed to be different then there is in some of the models evidence for a more extended structure with a height of 1.6 ± 0.8 $R_\odot$ (1×10^{11} cm) if it is on the G star, or $4.1^{+1.6}_{-0.9}$ $R_\odot$ (3×10^{11} cm) if it is on the K star.

In the χ^2 fitting the half-opening angles range between 10 and 40° on the G star and 3 and 40° on the K star. This translates to a maximum covering fraction of 26 ± 10% for the G star and $\sim$ 15% for the K star. The MEM maps give the most conservative estimate of the covering fractions. In the worst case 50% of the flux comes from 20% of the surface area of the star, although 10% is more typical.

4. DISCUSSION

The different orbital lightcurves seen above and below 1 keV in the ME and the LEIT provide direct evidence that the two temperature components discovered by Swank et al (1981) come from two physically distinct regions. The lack of any modulation at energies above 1 keV requires that the high temperature emission (> 10 million degrees) be located in such a way as to avoid a deep eclipse by the two stars. In contrast, the factor of two orbital modulation seen below 1 keV in the LEIT requires the presence of compact coronal structures on one or both stars with temperatures of < 10 million degrees. Three types of coronal structure are identified: 1) compact features with H< 10^{10} cm containing the cool component, 2) in some models extended structures with H $\sim$ 10^{11} cm, also containing the cool component, and 3) extended structures containing the hot component with a height that must large compared to that of the underlying stars, and probably pervades the whole binary system.

The measured temperature, T, and emission measure, EM=n_e^2 V, combine to give the pressure, P=$2n_e$kT, of the emitting plasma for a given volume, V. The results of the χ^2 fitting and MEM maps provide the first realistic limits on the volume filled by the low temperature component. The χ^2 fitting gives pressures in the compact regions that range from 100-450 dyne cm^{-2} for both stars. In the extended regions the pressure is a factor of 10-100 lower with a value of $\sim$ 15 dyne cm^{-2} on the G star and $\sim$ 4 dyne cm^{-2} on the K star. The dependence of the pressure on the height of the corona is illustrated in Figure 6 for each star using representative covering fractions of 20% and

https://doi.org/10.1017/S0252921100012318 Published online by Cambridge University Press

3%, and a typical emission measure of 1.0×10^{53} cm^{-3}. These pressure-height curves show how the average pressure increases for smaller covering fraction and height.

The range and distribution of the MEM derived pressures are in good agreement with those from the χ^2 fitting. The maximum entropy technique in general tries to provide images with the smallest range as possible of surface brightness (pressure) and can be considered as lower limits. For the compact emission on either star, the peak pressure of the various models ranged over 60–110 dynes cm^{-2}. The much larger heights of the extended emission components produced smaller peak pressures of 4–7 dynes cm^{-2}.

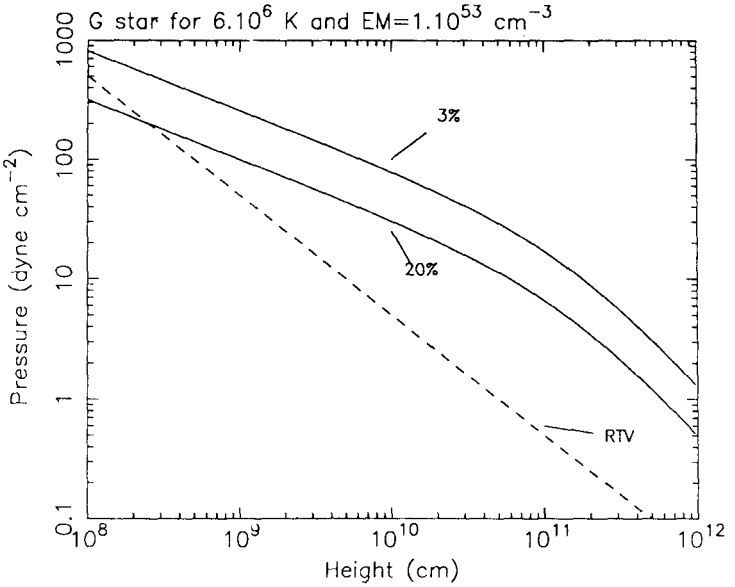

Figure 6. The solid lines indicate the relation between pressure and height for covering fractions of 3% and 20% for an emission measure of 1×10^{53} cm^{-3}. The dashed line shows that predicted by the RTV scaling law. These are for the G star, for the K star the solid lines are a factor of two lower, the dashed lines remain the same.

The limit set on the height of the compact corona of $< 1 \times 10^{10}$ $R_\odot$ is not very restrictive since it includes the dimensions of the entire range of structures found on the sun. However, in all cases the peak pressures for AR Lac stars are a factor of 10-100 higher than the quiescent sun. These pressures and the temperature of the cool component of $\sim 7 \times 10^6$ K are, however, similar to those found in solar flares. For the larger structures found in some of the AR Lac models the heights are comparable to the radius of the underlying star and also to the pressure scale height. While these larger loops are not required by all the models, the pressures are comparable with those found on the sun, but the dimensions are an order of magnitude larger.

The energy balance of a static, thermally insulated magnetic loop heated by an arbitrary energy source gives a scaling law between the half-length of the loop, L, and the peak temperature, T_p, and pressure of the form $T = 1.4 \times 10^3 (PL)^{1/3}$ (Rosner, Tucker and Vianna 1978, hereafter RTV). The EXOSAT results on AR Lac provide an opportunity to test the validity of this formulism in a stellar setting. The RTV relation is plotted on Figure 6 (assuming $L = \pi H/2$). The point where the RTV relation intercepts the pressure-height curves is within the upper limits on the height of the compact regions. Taken at face value the solutions require that for the models where the G

https://doi.org/10.1017/S0252921100012318 Published online by Cambridge University Press

star is bright the pressure is > 200 dyne cm^{-2} and the height $< 2,000$ km. For the models where the K star is bright the RTV relation gives pressures of > 70 dyne cm^{-2} with a height of $< 7,000$ km. The heights of a few thousand kilometers are reminiscent of X-ray bright points on the sun, although the pressure and temperature implied by the RTV relation are two orders of magnitude larger than in the solar case.

For the large extended structures where the height is resolved to be several solar radii the RTV relation does not intercept the pressure-height curves. The pressures are between 1 and 10 dynes cm^{-2}, comparable to the solar value, but the dimensions are an order of magnitude larger. Such a large discrepancy would require the loop height to be over 10 times the pressure or heating scale height to bring the RTV relation into agreement, which is unlikely (Serio et al 1981). We conclude that either the eclipse models that require these large structures are not correct, or that the energy input and balance for these large structures are very different from those of solar loops.

The radiative cooling times infered for both the compact and extended structures in AR Lac are similar to those found in the flaring sun. The cooling times of less than a 1000 s for the compact structures are much shorter than the assumed lifetime of the structures, and additional heating on a similar or shorter timescale is required to maintain the observed X-ray flux. For the extended structures the cooling time of 10,000 s (i.e. several hours) and hence the corresponding heating timescale required is also long.

We have concluded that the most likely explanation for the hot component is that it originates in large extended magnetic structures that pervade the whole system. The cooling time in such a large volume is of order of a day or longer. A puzzling aspect of the hot component is why the temperature of the plasma should be highest in the largest regions. This requires that the energy input increases with loop length, contrary to that generally assumed in the loop scaling law (e.g. RTV). A clue comes from the fact that the cooling time is of the order of a day or longer, such that a continuous energy source is not required. The only other occasion such high temperatures are seen is during flares where the total energy release can be up to $\sim 10^{35}$ erg (e.g. White et al 1986), a factor of ten more luminous than the two flares reported here. This energy may on occasions be channelled into heating plasma that escapes to a much larger volume. This might occur if during a large flare the plama broke out of its magnetic loop but was then trapped by other closed magnetic field lines further out. This might be expected if the flare was associated with a major reorganization of the magnetic field. Another possibility is that the larger scale magnetic field is constantly changing its configuration and releasing smaller energy impulses.

5. For the Future

The results of the modelling of the X-ray lightcurve of AR Lac have shown the power of eclipse observations to constrain the spatial structure of stellar coronae. The multiple solutions can be eliminated in future observations by making simultaneous high resolution uv observations of line profiles and using the doppler imaging technique to uniquely locate the chromospherically active regions (see Walter et al 1987, Vogt and Penrod 1983). The improvements in spectral resolution and collecting area given by future X-ray observatories such as XMM and AXAF will allow maps, such as those shown in Figures 4 and 5, to be made for individual spectral lines. By combining these with similar maps generated from uv and optical observations, which probe the upper and lower chromosphere, it will be possible to build a complete three dimensional view of the structure of stellar coronae.

6. REFERENCES

Chambliss, C.R. 1976, P.A.S.P., 88, 762.

Eaton, J., and Hall, D. 1979, Ap. J., 227, 907.

Majer, P., Schmitt, J.H.M.M., Golub, L., Harnden Jnr., F.R., and Rosner, R. 1986, Ap. J., 300, 360.

Mewe, R., Gronenschild, E.H.B.M., and van den Oord, G.H.J. 1985, Astr. Ap. Suppl., 62, 197.

Mewe, R., Schrijver, C.J., Lemen, J.R., and Bentley, R.D., 1986, Adv. Space Res., Vol. 6, No. 8, 133.

Rosner, R., Tucker, W. H., and Vaiana, G.S. 1978, Ap.J., 220, 643 (RTV).

Serio, S., Peres, G., Vaiana, G.S., Golub, L., and Rosner, R. 1981, Ap. J., 243, 288.

Skilling, J., and Bryan, R.K., 1984, M.N.R.A.S., 211, 111.

Stern, R.A., Antiochos, S.K. and Harnden, F.R. , 1986, Ap. J., 305, 417.

Swank, J.H., White, N.E., Holt, S.S., and Becker, R.H. 1981, Ap.J., 246, 214.

Vogt, S.S., and Penrod, G.D., 1983, P.A.S.P., 95, 565.

Walter, F.M., Gibson D.M., and and Basri, G.S. 1983, Ap.J., 267, 665 (WGB).

Walter, F.M., Neff, J.E., Gibson, D.M., Linsky, J.L., Rodono, M., Gary, D.E., and Butler, C.J. 1987, Astr. Ap., 186, 241.

White, N.E., Culhane, J.L., Parmar, A.N., Kellett, B.J., Kahn, S., van den Oord, and Kuijpers, J. 1986, Ap.J., 301, 262.

White, N.E., and Peacock, A.P. 1988, in *X-ray Astronomy with EXOSAT*, ed. N.E. White and R. Pallivicini, Memoria S.A.It, 59, in press.